

We are IntechOpen, the world's leading publisher of Open Access books Built by scientists, for scientists

6,900

Open access books available

186,000

International authors and editors

200M

Downloads

Our authors are among the

154

Countries delivered to

TOP 1%

most cited scientists

12.2%

Contributors from top 500 universities



WEB OF SCIENCE™

Selection of our books indexed in the Book Citation Index
in Web of Science™ Core Collection (BKCI)

Interested in publishing with us?
Contact book.department@intechopen.com

Numbers displayed above are based on latest data collected.
For more information visit www.intechopen.com



Progressive Failure Analysis of Glass/Epoxy Composites at Low Temperatures

Mohammad Amin Torabizadeh and
Abdolhossein Fereidoon

Additional information is available at the end of the chapter

<http://dx.doi.org/10.5772/55093>

1. Introduction

Fiber reinforced composite materials have been increasingly used as structural members in many structures such as airplane. The advantages of these materials are derived from their high strength, stiffness and damping together with low specific weight. Low temperature mechanical properties of glass fiber-reinforced epoxy have to be assessed, because of composite materials are subjected to low temperatures in service. Experimental or analytical investigation on the tensile failure behavior of glass/epoxy laminated composite with/or without stress concentration subjected to thermo-mechanical static loadings at low temperatures has not been done yet. In the present work, a model was developed to perform the progressive failure analysis of quasi isotropic composite plates at low temperatures. The initial failure load is calculated by means of an elastic stress analysis. The load is increased step by step. For each given load, the stresses are evaluated and the appropriate failure criterion is applied to inspect for possible failure. For the failed element, material properties are modified according to the failure mode using a non-zero stiffness degradation factor. Then, the modified Newton–Raphson iteration is carried out until convergence is reached. This analysis is repeated for each load increment until the final failure occurs and the ultimate strength is determined. The present method yields results in a reasonable agreement with the experimental data at room temperature and $-60\text{ }^{\circ}\text{C}$. The effect of low temperature on the failure mechanism of the plates was also determined.

2. Materials and mechanical testing

2.1. Material properties

Unidirectional glass fibers have been used in this investigation as reinforcing material, while epoxy resin has been utilized as the matrix material. Hand lay-up method was used to fabricate thin laminates with epoxy resin ML-506 with hardener HA11. Test specimens were cut from laminates according to relevant standard codes. All specimens had a constant cross section with tabs bonded to the ends. The fiber volume fraction of the composites was 55%.

2.2. Mechanical test equipments

The specimens are tested from beginning to the failure mode both at room and low temperatures. All tests were conducted under displacement control condition using Instron 5582 machine adaptable for cryogenic service by an environmental chamber. The displacement rate was 2 mm/min. Environmental chamber has the ability to cool down the temperature to -196°C by evaporating liquid cryogenic Nitrogen. During the tests, a pressurizing device is used to control the cooling time from room temperature to -20°C and -60°C and maintain an evaporating pressure of 152 kPa. In order to reach thermal equilibrium in mechanical parts of machine one hour prior to first time of testing, temperature of environmental chamber was kept at desired low temperatures. Since composite materials require more time than metal materials to reach thermal equilibrium states in low temperatures, specimens stayed in a constant low temperature for at least an hour prior to start loading. Environmental chamber was equipped with a fan to perform a uniform temperature. A digital thermometer was mounted inside of environmental chamber to monitor active temperature during the tests. Experimental set up for mechanical tests at different temperature is shown in Figure 1.

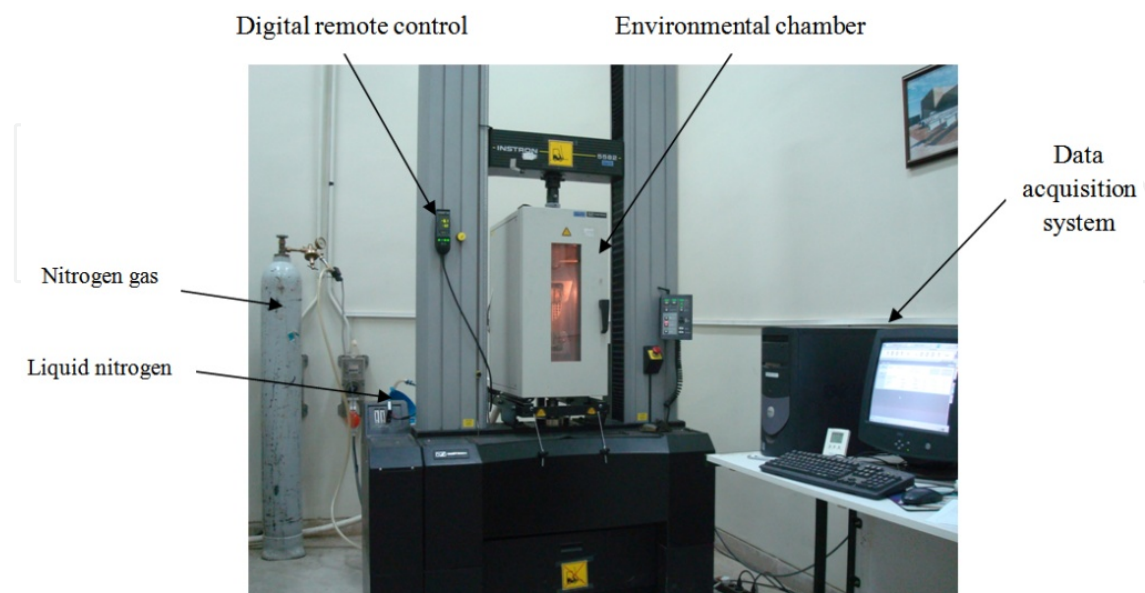


Figure 1. Experimental setup for mechanical tests at both room and low temperatures

3. Material characterization

In order to apply progressive damage modeling to a laminated composite, mechanical properties of unidirectional laminates should be assessed. For this purpose test specimens were fabricated for tensile, compressive and shear loading in longitudinal and transverse direction. In this section, for each case, specimen dimensions and experimental results are reported. Also some master curves are illustrated to predict mechanical properties in the assumed temperature range. Finally all of mechanical properties are assessed by a regression function.

3.1. Tensile test

The unidirectional glass fiber-reinforced epoxy which composed of ten plies was used in this test; the total thickness of the laminate is 2 mm. Unidirectional tensile specimens were cut out of the laminates in both fiber and matrix directions (longitudinal and transverse) according to ASTM D3039 [1]. Woven glass/epoxy tabs with tapered ends were locally bonded on each side of the specimens. These tabs allow a smooth load transfer from the grip to the specimen especially for low temperature test. The geometries of the specimens for longitudinal and transverse tensile tests are shown in Figure 2.

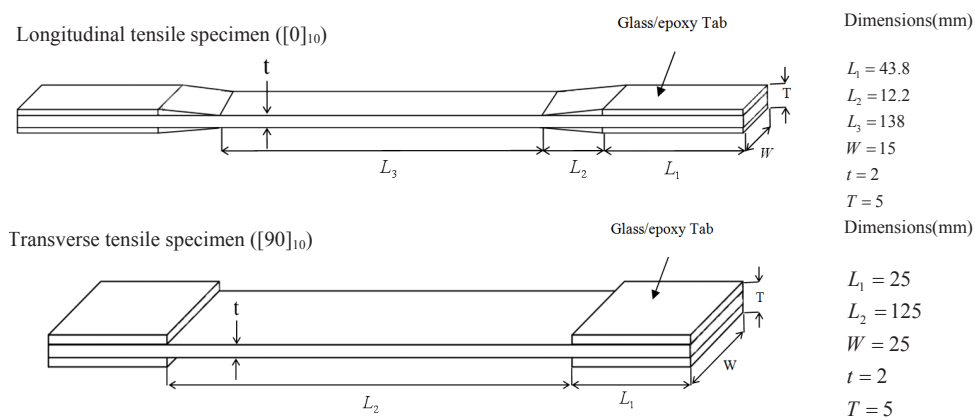


Figure 2. Geometry of the specimens for longitudinal and transverse tensile tests at different temperatures

The purpose of the static tensile tests was to determine the low temperature effects on the tensile strength, Young modulus and ultimate strain of unidirectional laminates in longitudinal and transverse directions. Figure 3 shows the typical stress-strain behavior of unidirectional laminate under tensile loads in longitudinal direction at room temperature, $-20\text{ }^\circ\text{C}$ and $-60\text{ }^\circ\text{C}$. The laminate exhibits a linear elastic behavior until breakage and the slope of the stress-strain curve increases as the temperature decreases. On the other hand, by decreasing temperature, strain to failure decreases slightly. The strain to failure reduction was very small (from 0.037, at room temperature, to 0.032 at $-60\text{ }^\circ\text{C}$). However, the strength and stiffness increase significantly as temperature decreases. The average value of tensile strength increases from 700.11 MPa, at room temperature, to 784.98 MPa, at $-60\text{ }^\circ\text{C}$, whereas the Young modulus also increases from 23.05 GPa at room temperature, to 28.65 GPa at $-60\text{ }^\circ\text{C}$. Some authors reported increasing of tensile strength and modulus for a UD glass-epoxy composite at cryogenic temperatures [10], [38]. Consequently, it was speculated that the brittleness of the fibers had

a major influence on the stiffness and strength increase of UD composites at low temperatures. Especially the brittleness of the fibers rapidly increased within a temperature range from RT to $-60\text{ }^{\circ}\text{C}$ which was indicated by Ref [10].

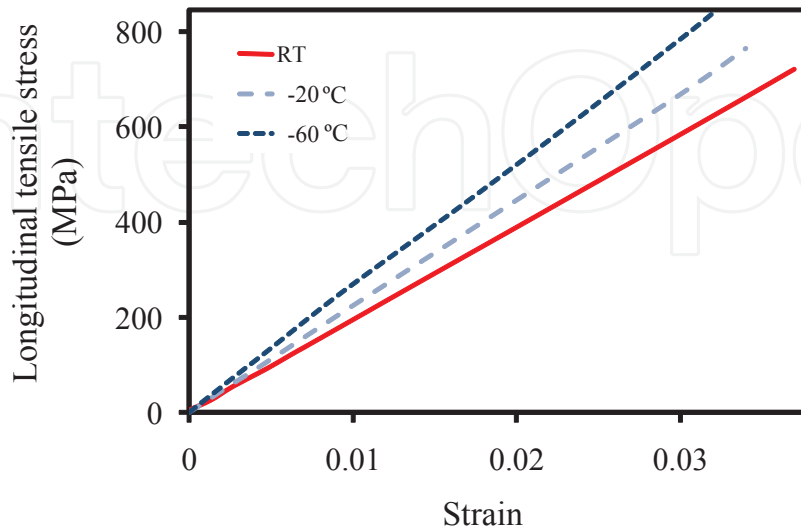


Figure 3. Typical stress-strain behavior of unidirectional laminate under tensile loads in longitudinal direction at room temperature, $-20\text{ }^{\circ}\text{C}$ and $-60\text{ }^{\circ}\text{C}$

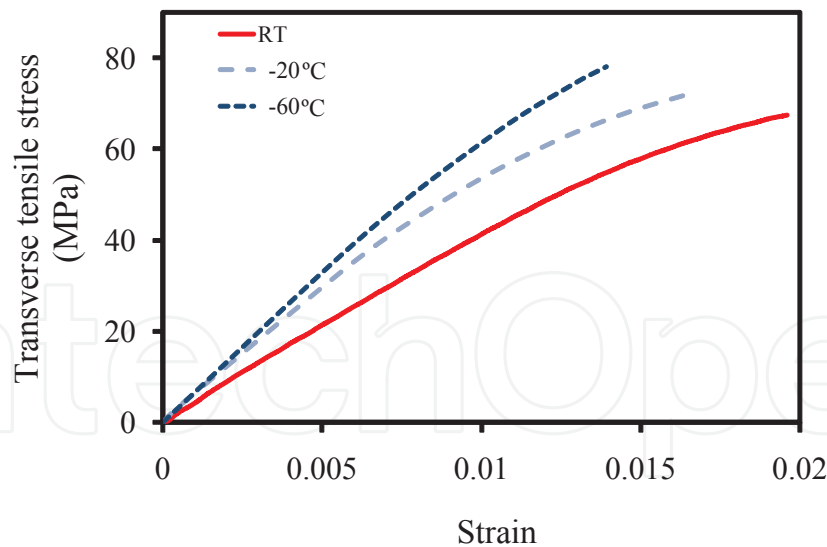


Figure 4. Typical stress-strain behavior of unidirectional laminate under tensile loads in transverse direction at room temperature, $-20\text{ }^{\circ}\text{C}$ and $-60\text{ }^{\circ}\text{C}$

Figure 4 show the load-deflection curve of unidirectional laminates under tensile loads in transverse direction. The behavior is the same as described in the previous tests. The only difference is that the stress-strain curve in this case showed insignificant nonlinearity before reaching the maximum stress, which is due to the nature of the plasticity of epoxy. It was

observed because the composite becomes more brittle in low temperatures, this nonlinearity behavior of matrix decreased by decreasing temperature in Figure 4 and Ref. [37]. Typical results was also reported that both transverse tensile strength and stiffness increased by decreasing temperature from RT for glass-epoxy composites [39].

Failure regions of the composite specimens at different temperatures in longitudinal and transverse directions under tensile loading are shown in Figure 5 and Figure 6 respectively. It is found that in the case of longitudinal tension, the failure mechanism changes with temperature while no significant change was observed on the transverse direction.

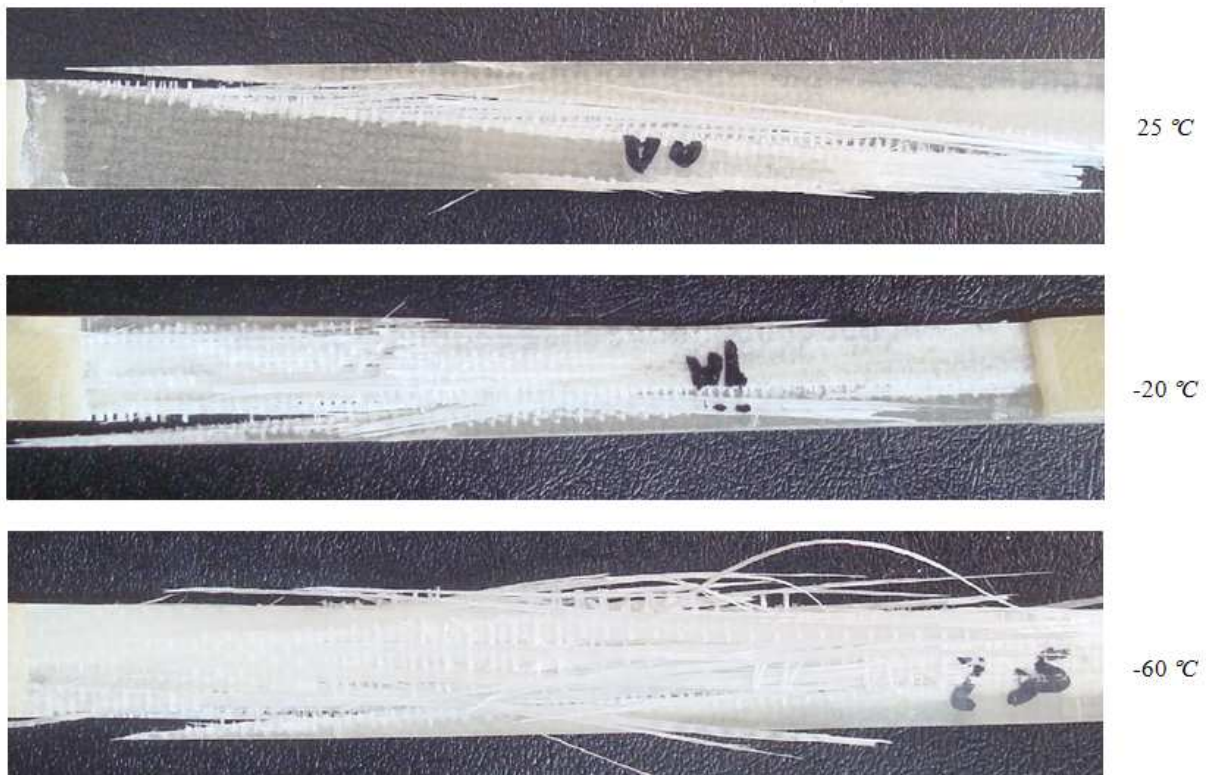


Figure 5. Failure regions of the composite specimens at different temperatures in longitudinal direction under tensile loading

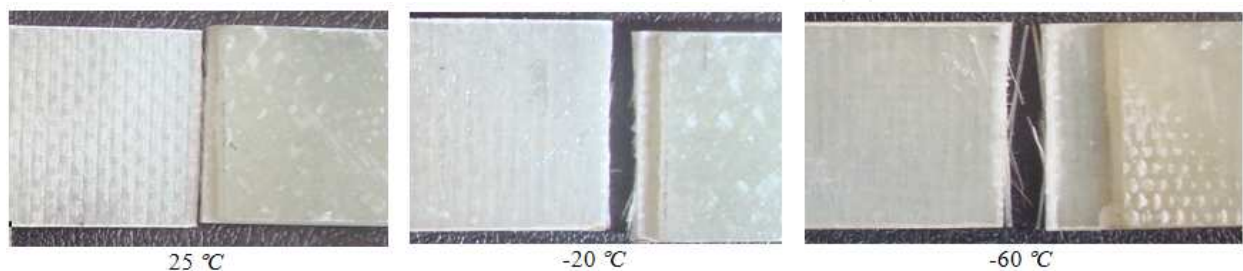


Figure 6. Failure regions of the composite specimens at different temperatures in transverse direction under tensile loading

For the longitudinal direction, from a visual inspection of the damage surfaces, a significant change could be observed in the fracture surface at room temperature to $-60\text{ }^{\circ}\text{C}$. There is a small amount of tab de-bonding near the gauge area for room temperature tested specimens. Also, fiber breakage which is more visible for low temperature case was occurred. At low temperature, due to weak interface between the fiber and matrix, fibers lose their bonds to the matrix. Moreover, matrix cracking and fiber pull-out were also observed. As shown in Figure 5, damage area was more limited at RT while by decreasing temperature to $-60\text{ }^{\circ}\text{C}$; the damage was extended further and covered the entire gauge region. In the transverse tension loading, net matrix failure observed near the gauge area. The major difference between room temperature and low temperatures tests in this case is that in low temperatures (Figure 6) small fiber-matrix debonding is observed which is not obvious in room temperature specimens. Also, bigger failure region of matrix is obvious at low temperatures. There is no significant change in failure mechanism for specimens at $-20\text{ }^{\circ}\text{C}$ and $-60\text{ }^{\circ}\text{C}$.

3.2. Compression test

The specimens used for compression test had the same material as those of the tensile test except that these specimens were made of fifteen plies so that the total thickness is 3 mm . Unidirectional compression specimens were cut in the longitudinal and transverse directions for longitudinal and transverse compression tests and also a fixture is used for the tests according to ASTM D3410 [2]. The geometries of the specimens are shown in Fig. 2. Woven glass/epoxy tabs were locally bonded on each side of the specimens to reduce the gripping effects. Also, a thin Teflon sheet, as a weakly bonded area, was inserted on each of the contacting surfaces between the specimens and the tabs to reduce the gripping effects in fiber compression specimens.

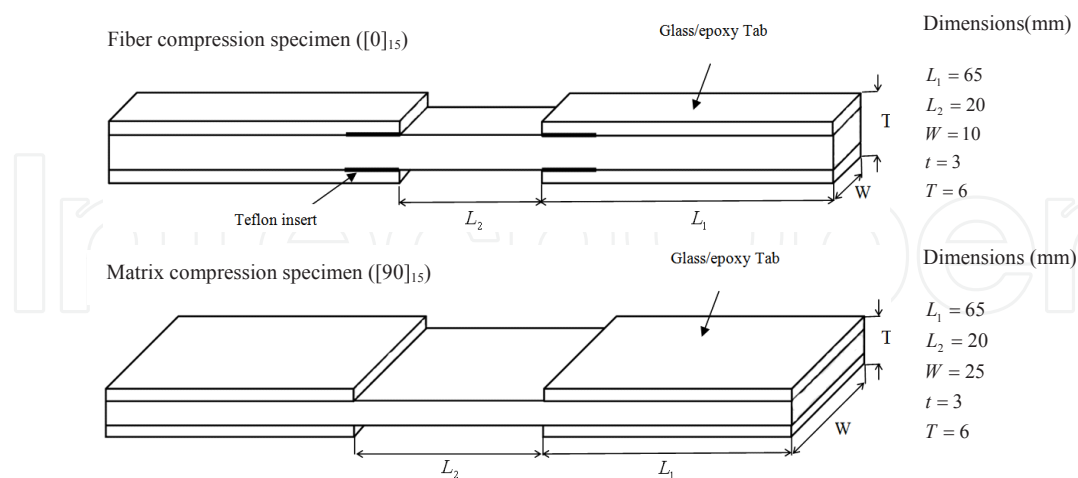


Figure 7. Geometry of the specimens for longitudinal and transverse compressive tests at different temperatures

In order to determine the effect of low temperature service on the strength and strain to failure of composite specimens in longitudinal and transverse directions, a set of experimental tests were performed. For this reason, a special fixture recommended in ASTM D3410 was used to

prevent possible buckling. Figure 8 illustrate typical stress-strain behavior of composite laminate under compressive loading in longitudinal direction at various temperatures. As shown, the stress-strain relation is slightly nonlinear and final failure occurs catastrophically in all cases. The main specific property of longitudinal compressive stress-strain curves is that against other nonlinear stress-strain curves of UD composite in longitudinal or transverse directions, these curves exhibit positive curvature. This may be due to interface bonding between matrix and fibers. Imperfect fiber-matrix bonding is a manufacturing defect that is created during curing process. This defect influences the role of the matrix that supports the fibers when the composite is under compression [28], [29]. From stress-strain curves, it seems that by increasing compression in longitudinal direction, this bonding becomes grater and the role of matrix against microbuckling of fibers is more highlighted. As shown in the figure, significant non-linear deformation was often observed before the maximum load [30], [31], and this behavior was associated to the plastic deformation of the polymeric matrix. Compressive strength in longitudinal direction increases significantly by decreasing temperature (from 570.37 MPa at room temperature, to 731.94 MPa at -60 °C).

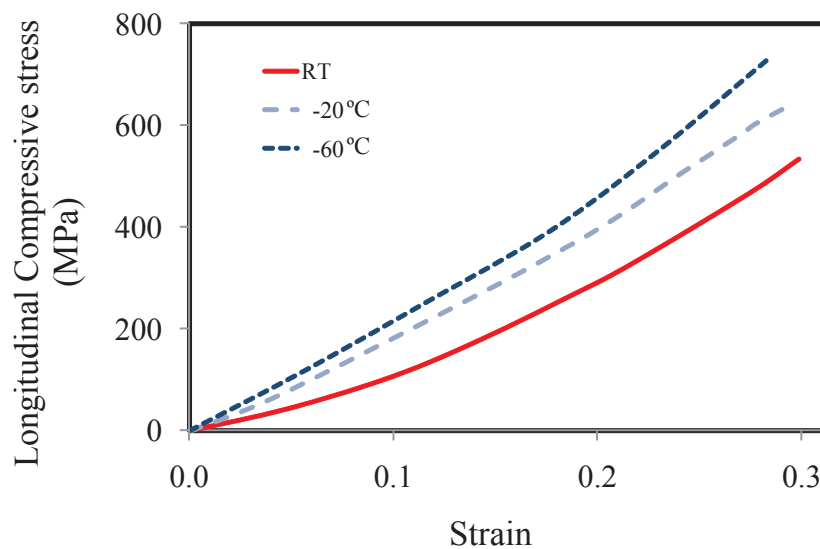


Figure 8. Typical stress-strain behavior of unidirectional laminate under compressive loads in longitudinal direction at room temperature, -20 °C and -60 °C

Figure 9 depict stress-strain curves of unidirectional composite under transverse compressive loading at different temperatures. Again significant increase in strength of composite was observed by decreasing temperature (from 122.12 MPa at room temperature, to 186.22 MPa at -60 °C). Typical behavior was reported by [32] for glass-epoxy composites. But in this case against other directions of loading, by decreasing temperature, transverse compressive stiffness was decreased and strain to failure was increased significantly. The reason of the observed phenomenon in this type of loading is unknown and it is interested to investigate more about this behavior in future works.

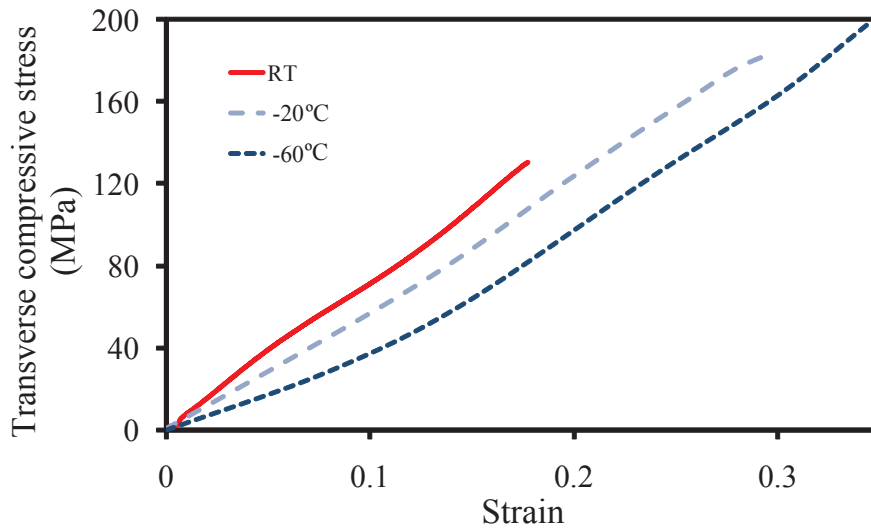


Figure 9. Typical stress-strain behavior of unidirectional laminate under compressive loads in transverse direction at room temperature, -20 °C and -60 °C

Figure 10 and Figure 11 show failed specimens under compressive loading in longitudinal and transverse directions at different temperatures, respectively.

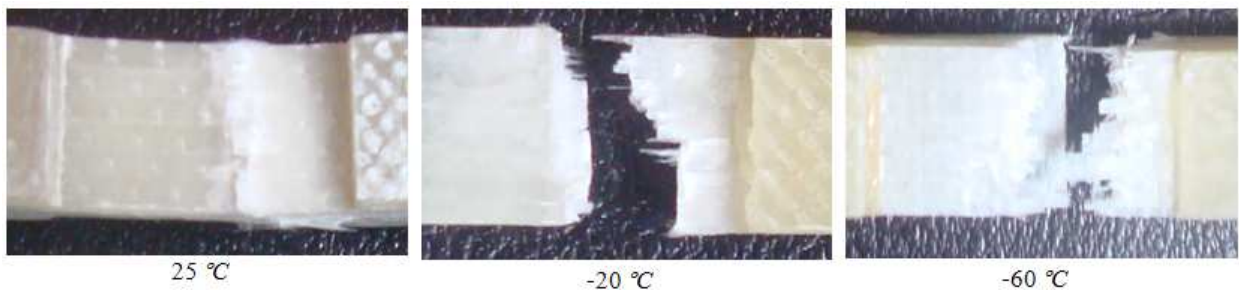


Figure 10. Failure regions of the composite specimens at different temperatures in longitudinal direction under compressive loading

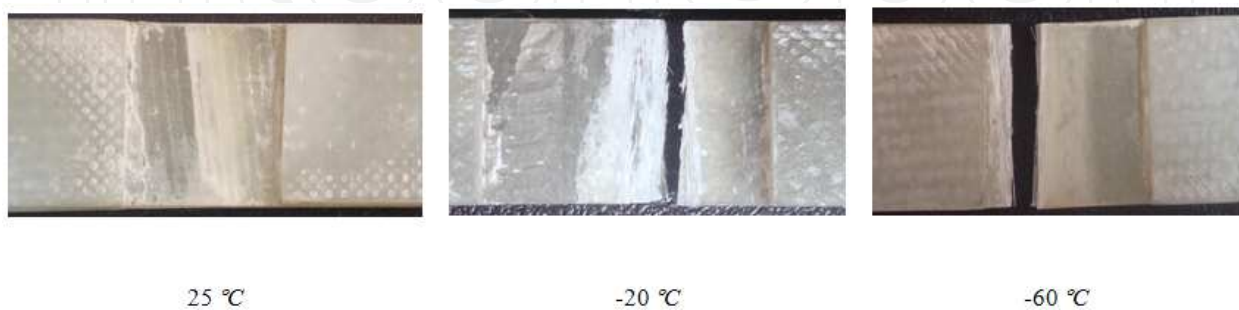


Figure 11. Failure regions of the composite specimens at different temperatures in transverse direction under compressive loading

The main failure mode of specimens in this case is micro buckling of fibers in shear or extensional mode. Also, in this case, there is a small amount of tab deboning near the gauge area for room temperature specimens. The change in the mechanical response with decreasing temperature is associated with a change in failure modes. As shown in Figure 11, failure occurred at the middle of specimen under micro-buckling failure mode. The difference is that, in low temperature cases, more fiber pull-out was occurred. Also, extensive deboning between fibers and the matrix was also observed because of weaker fiber and matrix bonding at low temperatures. In this case, only at low temperatures failed specimens fractured in two separate parts. In the case of compression failure in the transverse direction at low temperature, the failure area is much more than the room temperature specimens. Also at room temperature, specimen is not fractured in two separate parts. This is because of major effects of low temperature on mechanical properties of epoxy matrix of composites. In this case, there is no significant change in failure mechanism for specimens at -20°C and -60°C . It is found the role played by two dominant damage mechanisms (decohesion at the interface and shear band formation in the matrix) in controlling the composite strength. On the other hand, if decohesion is inhibited, failure took place by the development of shear bands in the matrix which propagated through the microstructure at angle of $\pm 45^{\circ}$ with respect to the plane perpendicular to the compression axis [32]. The compressive strength was slightly higher than the matrix strength under compression due to the additional strengthening provided by the fibers. Parametric studies showed that other factors (such as the matrix friction angle, the interface fracture energy and the thermo-elastic residual stresses) exerted a secondary influence on the compressive strength of PMC under transverse compression [32]. But the matrix is more susceptible to the formation of shear bands. The angle formed between the failure plane and in-plane loading direction is slightly above 45° and typical values reported are in the range $50\text{-}56^{\circ}$ [40]-[42].

3.3. In-plane shear test

In the following, method of static experiments for characterizing material properties under in-plane shear loading is illustrated. Among numerous testing methods, the three-rail shear test method, described by the ASTM A4255 [3], is a fairly reliable technique. This method is modified by Shokrieh [28]. He developed new specimen by inserting notches into the edges of specimen. The reason behind the insertion of notches at the locations of stress concentrations is to replace a very sharp crack with a blunt crack with much lower stress concentration factor. To increase the stability of the specimen during the test, a $[0,90]_s$ configuration is selected in this test. The specimen and the dimension are shown in Figure 12.

Electric strain gauges were used to measure the strains of the specimens during the shear tests. The strain gauges are attached to the specimens in the direction of 45° . The strain gauges and lead wires were manufactured by TML Corporation for low temperature ranges. However, since the changing in temperature would also affect the strain in strain gauges, Wheatstone half bridge circuit has been used to reduce this unfavorable effect.

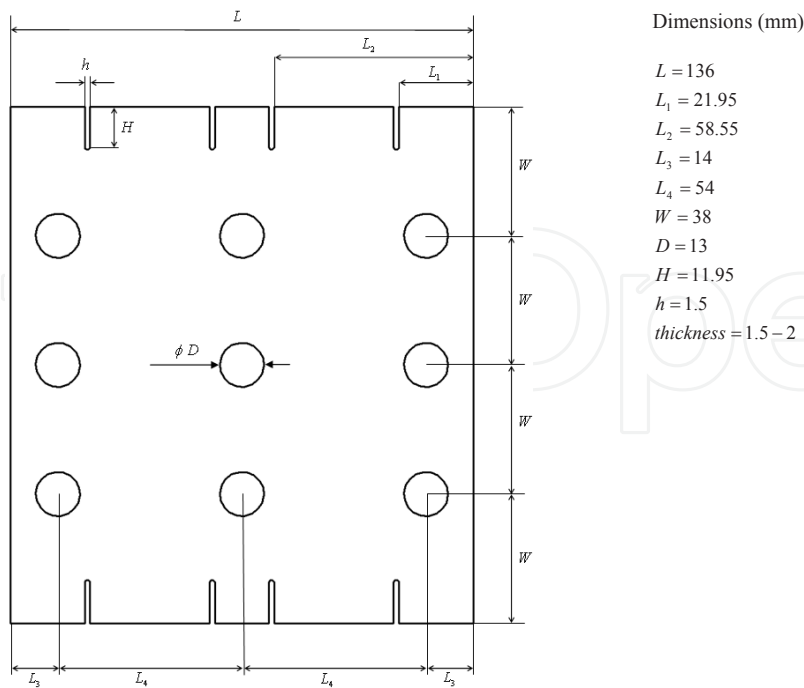


Figure 12. Geometry of the specimens for in-plane shear tests at different temperatures

Figure 13 show the stress-strain behavior of modified specimen under in-plane shear loadings at room temperature, $-20\text{ }^{\circ}\text{C}$ and $-60\text{ }^{\circ}\text{C}$. As shown, this behavior is highly nonlinear for all temperature tests. Also, as temperature decreases to $-60\text{ }^{\circ}\text{C}$ from the room temperature, both the in-plane shear modulus and strength increased significantly.

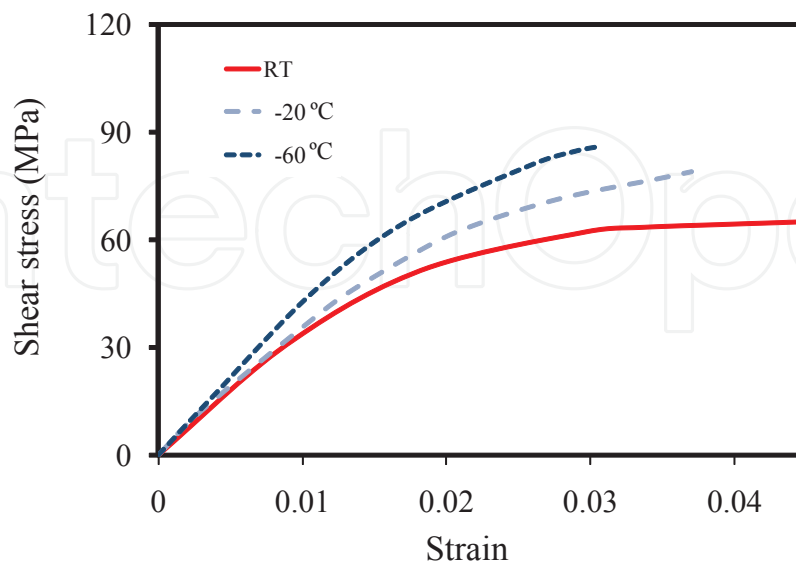


Figure 13. Typical stress-strain behavior of unidirectional laminate under in-plane shear loading at room temperature, $-20\text{ }^{\circ}\text{C}$ and $-60\text{ }^{\circ}\text{C}$

For metallic materials, the linear region of the stress-strain curve corresponds to elastic deformation and the nonlinear region to plastic deformation. However, when working with non-crystalline substances (such as epoxy), the glass transition temperature (T_g) determines whether a material can exhibit viscous, or non-linear, behavior. Below the glass transition temperature a non-crystalline material is considered an amorphous solid, above it a rubbery solid and, as the temperature increases, a viscous liquid [33]. A non-crystalline material such as a polymer can only exhibit viscous behavior above T_g ; below T_g , the material will fail before it plastically deforms. All of the tests in the current study were conducted well below T_g for the epoxy resin (≈ 157 °C). This indicates that the nonlinear regions of the shear stress-shear strain curves generated by the tests at room and low temperatures are not the result of viscous, or plastic, deformation [37]. This nonlinear behavior is thought to be the result of micro-crack accumulation throughout the matrix. The extensive nonlinear region displayed in the room temperature stress-strain curves would correspond to a high density of micro-cracks throughout the material (Figure 13). The more limited nonlinear region in the curves generated from the tests done at low temperatures imply that there is a progressive decrease in micro-crack accumulation within the specimen with decreasing temperature. Reduction the nonlinear region of stress-strain curves at low temperatures also confirmed by a suitable candidate model to study the nonlinear behavior of composites under shear loading which was proposed by Hahn and Tsai [28]. Parameter of material nonlinearity decreased from $1.76e^{-8}$ MPa⁻³ at room temperature to $1.33e^{-8}$ MPa⁻³ at -60 °C. Figure 14 show tested specimens and failure regions under in-plane shear loading at different temperatures. As shown in the figure, more damaged area was observed with decreasing temperature from room temperature to -60 °C.

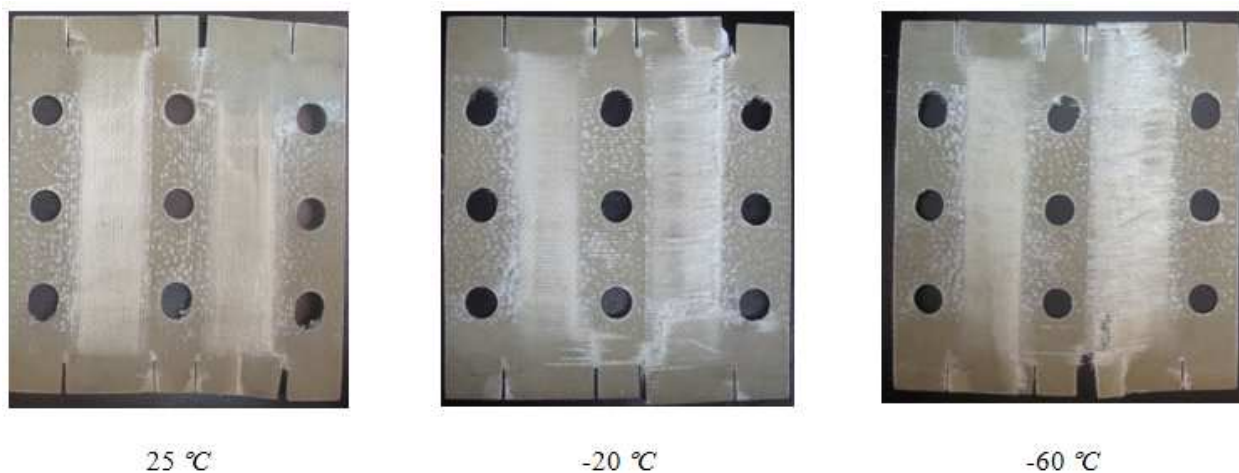


Figure 14. Tested specimens under shear loading at different temperatures

3.4. Master curves for mechanical properties

Figure 15 show the experimental values of tensile and compressive strengths for unidirectional laminates at different temperatures in longitudinal and transverse directions with their calculated standard deviations.

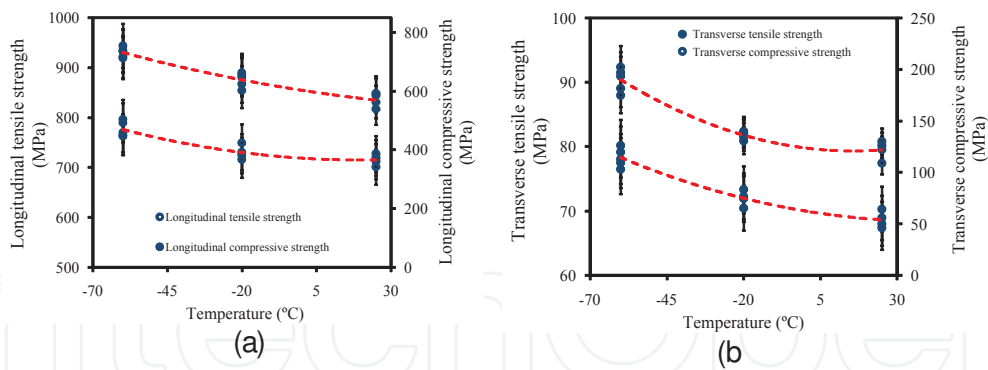


Figure 15. Experimental values of the tensile and compressive strengths for unidirectional laminates at different temperature in a) longitudinal and b) transverse directions

In each case in the above figures, by a polynomial curve fitting to experimental data, the increasing trend of strengths by decreasing the temperature is shown. However, the increasing rate of compressive strength by decreasing temperature is more for that of the tensile strength in both longitudinal and transverse directions. Figure 16 show experimental values of tensile modulus for unidirectional laminates at different temperatures in longitudinal and transverse directions. Both longitudinal and transverse tensile modulus increased by decreasing temperature to -60°C .

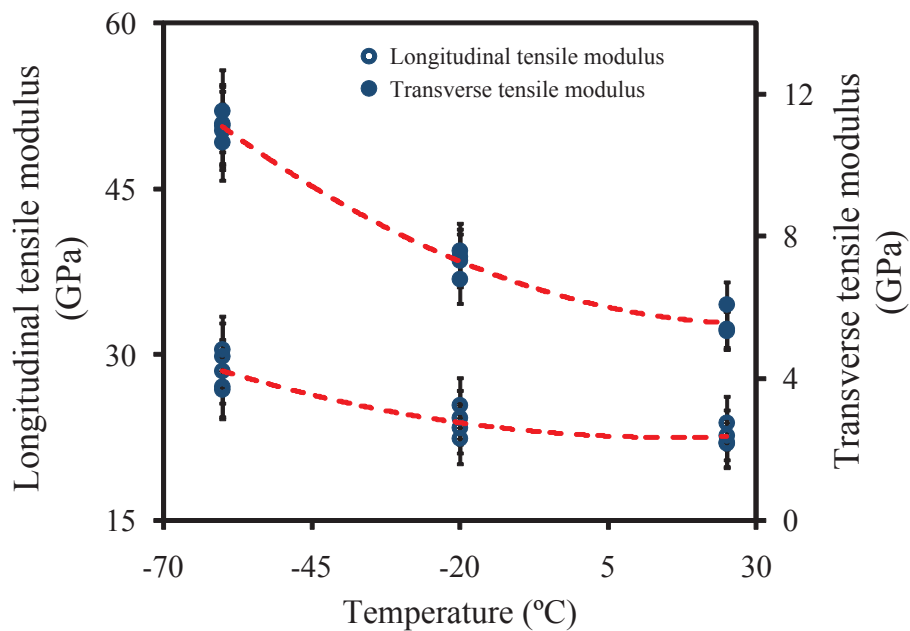


Figure 16. Experimental values of tensile modulus for unidirectional laminates at different temperature in longitudinal and transverse directions

Decreasing temperature, in this case, has lower effect on the final failure mode of the compression tests of the unidirectional plies in longitudinal and transverse directions at various temperatures in comparison with the previous one. Experimental magnitudes of shear strength

and modulus at different temperatures are compared in Figure 17. In the case of shear loading, low temperature has major effect on mechanical properties of composites.

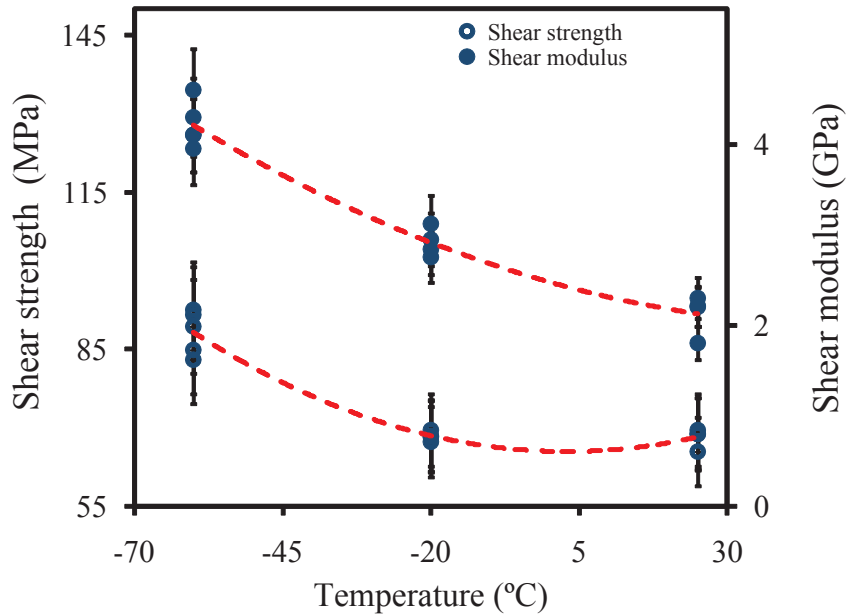


Figure 17. Experimental values of shear strength and modulus for cross ply laminates at different temperatures

Temperature effects on mechanical properties of UD composites which are plotted in Figure 15 to Figure 17 can be assessed also using a regression function defined by:

$$M(T) = \alpha T^2 - \beta T + \gamma$$

where, M and T are the mechanical property and temperature, respectively. Also α , β and γ are the material constants. The values for α , β , γ and R (the correlation coefficient) are given in Table 1.

| Material constants | α | β | γ | R |
|-----------------------------------|----------|---------|----------|--------|
| Longitudinal compressive strength | 0.0093 | 1.5706 | 604.05 | 0.9575 |
| Transverse compressive strength | 0.0121 | 0.3784 | 124.04 | 0.9678 |
| Longitudinal tensile strength | 0.0098 | 0.3808 | 718.52 | 0.9642 |
| Transverse tensile strength | 0.0010 | 0.0789 | 70.390 | 0.9622 |
| In-plane shear strength | 0.0058 | 0.0341 | 65.339 | 0.9682 |
| Longitudinal modulus | 0.0011 | 0.0326 | 22.800 | 0.9666 |
| Transverse modulus | 0.0007 | 0.0420 | 6.1913 | 0.9920 |
| In-plane shear modulus | 0.0002 | 0.0184 | 2.477 | 0.9769 |

Table 1. Material constants and correlation coefficients $-60\text{ }^\circ\text{C} \leq T \leq 23\text{ }^\circ\text{C}$

4. Specimen geometry

Quasi-isotropic lay-up ($[0/\pm 45/90]_{2s}$) was used in this study for tensile tests at room temperature and -60°C . For this reason, thin laminate composed of ten plies of reinforcement with epoxy resin were fabricated with considered configuration, giving a laminate approximately 2 mm in thickness. For laminate with stress concentration, a central hole was made by a machine. Woven glass/epoxy tabs with tapered ends were locally bonded on each side of the specimens. These tabs allow a smooth load transfer from the grip to the specimen especially for low temperature test. All specimens had a constant cross section with tabs bonded to the ends. The geometry of the specimen with stress concentration for tensile tests is shown in Figure 18.

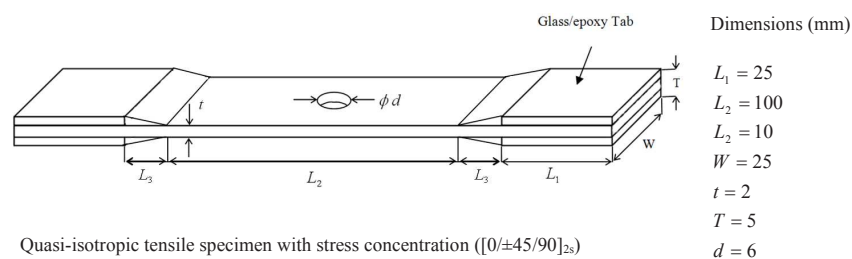


Figure 18. Geometry of the specimen with stress concentration for tensile test at room temperature and -60°C

5. Progressive Damage Modeling (PDM)

5.1. Stress analysis

The first component of the PDM is finite element stress analysis. Consider a composite plate with/without stress concentration (Figure 18). The plate has width $w = 25$ mm, length $l = 170$ mm, thickness $t = 2$ mm and central hole $D = 6$ mm (if applicable). The plate is a laminated composite with quasi-isotropic ply orientation. A two dimensional macro code by APDL of ANSYS [33] is developed to perform finite element analysis. In this paper, the 8-node layered element SHELL 99 is adopted to model the laminates, which allows up to 250 different material layers in the thickness direction in each element without much increase of counting time. Mechanical properties of a unidirectional laminate at room temperature and -60°C , which is used as initial values in FEM and listed in Table 2, were tested by the present authors [34].

In this table, the script x refers to the fiber direction, and y refers to direction perpendicular to the fiber direction. In this study, the stress resultants are defined as follow:

$$\sigma_{Total} = \sigma_M + \sigma_T \quad (1)$$

| Mechanical properties | 23 °C | -60 °C |
|---|--------|--------|
| Longitudinal modulus E_x (GPa) | 19.94 | 28.65 |
| Transverse modulus E_y (GPa) | 5.83 | 11.03 |
| Shear modulus G_{xy} (GPa) | 2.11 | 4.21 |
| Longitudinal tensile strength X_t (MPa) | 700.11 | 784.98 |
| Longitudinal compression strength X_c (MPa) | 570.37 | 731.94 |
| Transverse tensile strength Y_t (MPa) | 69.67 | 75.2 |
| Transverse compression strength Y_c (MPa) | 122.12 | 186.22 |
| Shear strength S (MPa) | 68.89 | 91.22 |

Table 2. Mechanical properties of GFRP at room and low temperatures

where σ_M and σ_T are the mechanical and thermal stresses respectively. Thermal stresses are due to decreasing temperature from room temperature to -60 °C. These stress resultants will be calculated by the following relation:

$$\sigma_T = \begin{Bmatrix} \sigma_x^T \\ \sigma_y^T \\ \sigma_{xy}^T \end{Bmatrix} = \begin{bmatrix} \bar{Q}_{11} & \bar{Q}_{12} & \bar{Q}_{16} \\ \bar{Q}_{21} & \bar{Q}_{22} & \bar{Q}_{26} \\ \bar{Q}_{61} & \bar{Q}_{62} & \bar{Q}_{66} \end{bmatrix} \begin{Bmatrix} \varepsilon_x^T \\ \varepsilon_y^T \\ \gamma_{xy}^T \end{Bmatrix} \quad (2)$$

In the above equation, $[\bar{Q}_{ij}]$ is transformed reduced stiffness matrix for a laminated composite and $\{\varepsilon_{ij}^T\}$ is thermal strain vector which is defined as follow:

$$\begin{Bmatrix} \varepsilon_x^T \\ \varepsilon_y^T \\ \gamma_{xy}^T \end{Bmatrix} = \Delta T \begin{Bmatrix} \alpha_x \\ \alpha_y \\ \alpha_{xy} \end{Bmatrix} \quad (3)$$

where ΔT and $\{\alpha_{ij}\}$ are temperature difference from room temperature and coefficients of thermal expansion for an angle ply laminate, respectively. $\{\alpha_{ij}\}$ can be given in terms of the coefficients of thermal expansion for a unidirectional laminate as:

$$\begin{Bmatrix} \alpha_x \\ \alpha_y \\ \alpha_{xy} / 2 \end{Bmatrix} = [T]^{-1} \begin{Bmatrix} \alpha_1 \\ \alpha_2 \\ 0 \end{Bmatrix} \quad (4)$$

and $[T]$ is a transformation matrix for an angle ply laminate [35].

5.2. Failure criterion

The second part of PDM is failure analysis. By using finite element results, at layer level in each element, stiffness reduction is carried out considering five types of damages: fiber and matrix in tension and compression and fiber-matrix shearing modes. To detect them, a set of two dimensional stress based failure criterion is selected. The following Hashin criteria [28] are used to detect five different failure modes. The first two of the failure modes are catastrophic and the others are not.

| Condition | Failure criteria | Failure relation |
|---|-------------------------------|-------------------|
| $\left(\frac{\sigma_{xx}}{X_t}\right)^2 + \left(\frac{\sigma_{xy}}{S}\right)^2 = e_{F^+}^2 \begin{cases} e_{F^+} \geq 1 & \text{Fail} \\ e_{F^+} < 1 & \text{Safe} \end{cases}$ | Fiber tensile failure | $\sigma_{xx} > 0$ |
| $\left(\frac{\sigma_{xx}}{X_c}\right) = e_{F^-} \begin{cases} e_{F^-} \geq 1 & \text{Fail} \\ e_{F^-} < 1 & \text{Safe} \end{cases}$ | Fiber compressive failure | $\sigma_{xx} < 0$ |
| $\left(\frac{\sigma_{yy}}{Y_t}\right)^2 + \left(\frac{\sigma_{xy}}{S}\right)^2 = e_{M^+}^2 \begin{cases} e_{M^+} \geq 1 & \text{Fail} \\ e_{M^+} < 1 & \text{Safe} \end{cases}$ | Matrix tensile failure | $\sigma_{yy} > 0$ |
| $\left(\frac{\sigma_{yy}}{Y_c}\right)^2 + \left(\frac{\sigma_{xy}}{S}\right)^2 = e_{M^-}^2 \begin{cases} e_{M^-} \geq 1 & \text{Fail} \\ e_{M^-} < 1 & \text{Safe} \end{cases}$ | Matrix compressive failure | $\sigma_{yy} < 0$ |
| $\left(\frac{\sigma_{xx}}{X_c}\right)^2 + \left(\frac{\sigma_{xy}}{S}\right)^2 = e_{FM}^2 \begin{cases} e_{FM} \geq 1 & \text{Fail} \\ e_{FM} < 1 & \text{Safe} \end{cases}$ | Fiber-Matrix shearing failure | $\sigma_{xx} < 0$ |

Table 3. Hashin failure criterion

5.3. Material properties degradation rules

The last component of PDM is material properties degradation. As failure occurs in a unidirectional ply of a laminate, material properties of that failed ply are changed by a set of sudden material property degradation rules. In the present method after failure occurrence in a ply of the laminate, instead of inducing real crack, the failed region of the unidirectional ply is replaced by an intact ply of lower material properties. A complete set of sudden material property degradation rules for all various failure modes of a unidirectional ply under a uniaxial static stress is explained in the following. The rules must be carefully applied to avoid numerical instabilities during computation by the computer program.

- Fiber tension failure

Fiber tension failure mode of a ply is a catastrophic mode of failure and when it occurs, the failed material cannot sustain any type or combination of stresses. Thus, all material properties of the failed ply are reduced, as follows:

$$\left[E_x, E_y, G_{xy}, \nu_{xy}, \nu_{yx} \right] \rightarrow \left[\lambda_{cdr} E_x, \lambda_{cdr} E_y, \lambda_{cdr} G_{xy}, \lambda_{cdr} \nu_{xy}, \lambda_{cdr} \nu_{yx} \right] \quad (5)$$

$$\left[X_t, Y_t, X_c, Y_c, S \right] \rightarrow \left[\lambda_{cdr} X_t, \lambda_{cdr} Y_t, \lambda_{cdr} X_c, \lambda_{cdr} Y_c, \lambda_{cdr} S \right] \quad (6)$$

where λ_{cdr} is coefficient of degradation rules. Extensive comparative studies are carried out to study the effect of λ_{cdr} , which indicates that λ_{cdr} would greatly influence the strength prediction and failure mechanism in the progressive damage model. After a careful comparative study, $\lambda_{cdr}=0.001$ is applied in the current model.

- Fiber compression failure

Fiber compression failure mode of a unidirectional ply is a catastrophic mode of failure and when it occurs, the failed material cannot sustain any type or combination of stresses. Thus, all material properties of the failed ply are reduced. Equations 7 and 8 show this degradation rule.

$$\left[E_x, E_y, G_{xy}, \nu_{xy}, \nu_{yx} \right] \rightarrow \left[\lambda_{cdr} E_x, \lambda_{cdr} E_y, \lambda_{cdr} G_{xy}, \lambda_{cdr} \nu_{xy}, \lambda_{cdr} \nu_{yx} \right] \quad (7)$$

$$\left[X_t, Y_t, X_c, Y_c, S \right] \rightarrow \left[\lambda_{cdr} X_t, \lambda_{cdr} Y_t, \lambda_{cdr} X_c, \lambda_{cdr} Y_c, \lambda_{cdr} S \right] \quad (8)$$

As mentioned, these two modes of failure are catastrophic, therefore if it occurs, the other modes of failure do not need to also be verified.

- Matrix tension failure

In matrix tension failure mode of a ply, that is not catastrophic failure, only matrix direction affected, therefore other material properties are left unchanged. (Eq. 9 and 10)

$$\left[E_x, E_y, G_{xy}, \nu_{xy}, \nu_{yx} \right] \rightarrow \left[E_x, \lambda_{cdr} E_y, G_{xy}, \nu_{xy}, \lambda_{cdr} \nu_{yx} \right] \quad (9)$$

$$\left[X_t, Y_t, X_c, Y_c, S \right] \rightarrow \left[X_t, \lambda_{cdr} Y_t, X_c, Y_c, S \right] \quad (10)$$

- Matrix compression failure

Matrix compression failure mode results in the same type of damage to the composite ply as the matrix tension failure mode. This mode of failure is not catastrophic; therefore, other material properties are left unchanged:

$$\left[E_x, E_y, G_{xy}, \nu_{xy}, \nu_{yx} \right] \rightarrow \left[E_x, \lambda_{cdr} E_y, G_{xy}, \nu_{xy}, \lambda_{cdr} \nu_{yx} \right] \quad (11)$$

$$[X_t, Y_t, X_c, Y_c, S] \rightarrow [X_t, Y_t, X_c, \lambda_{cdr} Y_c, S] \quad (12)$$

- Fiber-Matrix shear failure

In fiber-matrix shearing failure modes of a ply, the material can still carry load in the fiber and matrix directions, but in-plane shear stress can no longer be carried. This is modeled by reducing the in-plane shear material properties of the failed ply, as follows:

$$[E_x, E_y, G_{xy}, \nu_{xy}, \nu_{yx}] \rightarrow [E_x, E_y, \lambda_{cdr} G_{xy}, \lambda_{cdr} \nu_{xy}, \lambda_{cdr} \nu_{yx}] \quad (13)$$

$$[X_t, Y_t, X_c, Y_c, S] \rightarrow [X_t, Y_t, X_c, Y_c, \lambda_{cdr} S] \quad (14)$$

The PDM is an integration of the three important components: stress analysis, failure analysis and material property degradation. The model is capable of simulating the first and final failure load of composite laminates with arbitrary geometry and stacking sequence under tensile static loading at room temperature and -60°C .

A computer program, the algorithm of which is shown in Figure 19, is established to analyze the failure mechanism of composite plates at low temperatures using APDL of ANSYS. All material properties are set to initial values which are experimentally evaluated by present authors [34]. The initial failure load is calculated by means of an elastic stress analysis. The load is increased step by step. For each given load, the stresses at each integration point are evaluated and the appropriate failure criterion is applied to inspect for possible failure. At the point with failure, the material properties are modified according to the failure mode using a non-zero stiffness degradation factor. Then, the modified Newton–Raphson iteration is carried out until convergence is reached. The convergence tolerance is assumed to be 0.001. This analysis is repeated for each load increment until the final failure occurs and the ultimate strength is determined.

Theoretically, the smaller load increment between successive steps, the more accurate analysis result can be achieved. However, a reasonable load increment should be prescribed to avoid too much analysis time and to ensure accuracy. After sensitivity analysis on load increment, 1 KN is applied in the current model.

6. Results and discussion

The specimens are tested under static tensile loading at room and low temperatures. In each case (with or without stress concentration) at room temperature four specimens and at -60°C five coupons were tested to show statistic scatter of experiments. By statistical evaluation (mean values and standard deviation) reliability of results were appraised. The experimental setup for low temperature tests using an environmental chamber is shown in Figure 20.

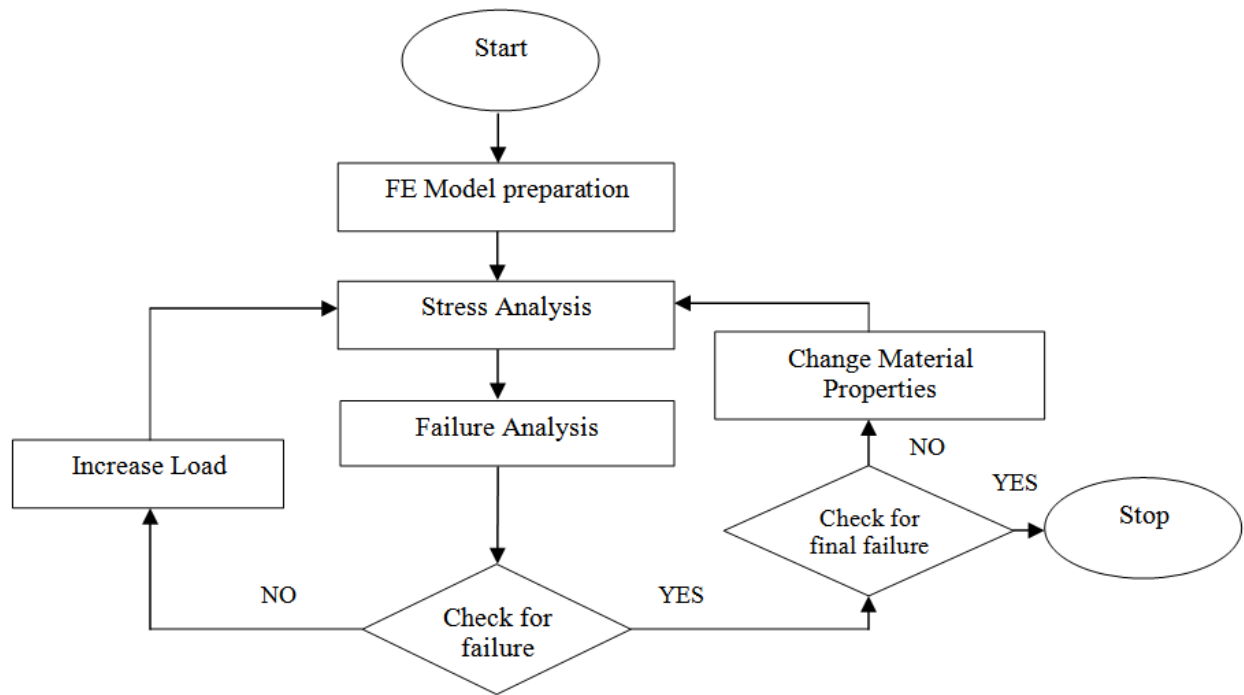


Figure 19. The algorithm of progressive damage modeling

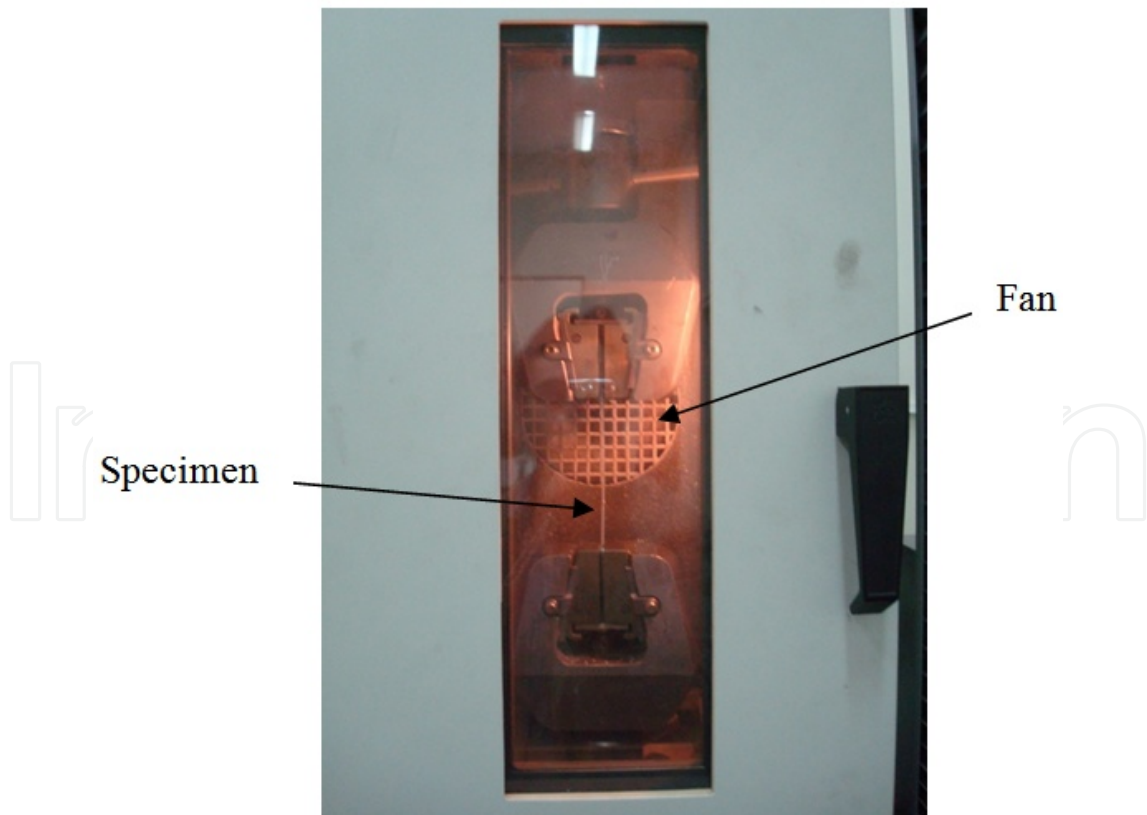


Figure 20. Environmental chamber for low temperature tests

The average tensile properties such as first ply failure (FPF) load, final failure (FF) load and ultimate strain to failure (USF) for quasi-isotropic laminates with/without stress concentration determined based on results of stress–strain curves from experimental tests and numerical analysis are summarized in Table 4.

| | With stress concentration | | | | Without stress concentration | | | |
|----------|---------------------------|-------|--------------|-------|------------------------------|-------|--------------|-------|
| | Analytical | | Experimental | | Analytical | | Experimental | |
| | RT | -60°C | RT | -60°C | RT | -60°C | RT | -60°C |
| FPF (KN) | 2.045 | 6.28 | 1.8 | 5.75 | 3.12 | 5.62 | 2.15 | 4.52 |
| FF (KN) | 13.72 | 18.27 | 11.96 | 16.31 | 15.58 | 18.53 | 13.86 | 17.37 |
| USF | 0.041 | 0.036 | 0.040 | 0.037 | 0.056 | 0.058 | 0.055 | 0.057 |

Table 4. Average test results on glass/epoxy laminated composite at room temperature and -60 °C

Figure 21 and Figure 22 show the failure process predicted by the model at room temperature and -60 °C, respectively. At the FPF load, a mainly obvious damage around the hole of plate is matrix cracking (see Figure 21a and Figure 22a). By increasing the load, other failure modes are also occurred (see Figure 21b and Figure 22b). At the final failure load, the plate breaks along the transverse direction through the central hole edge, the same as noticed in the experimental tests. In this load, the mainly failure mode is fiber breakage (see Figure 21c and Figure 22c). As shown in the following figures, the failure regions of specimens at -60 °C at each step is much more than room temperature.

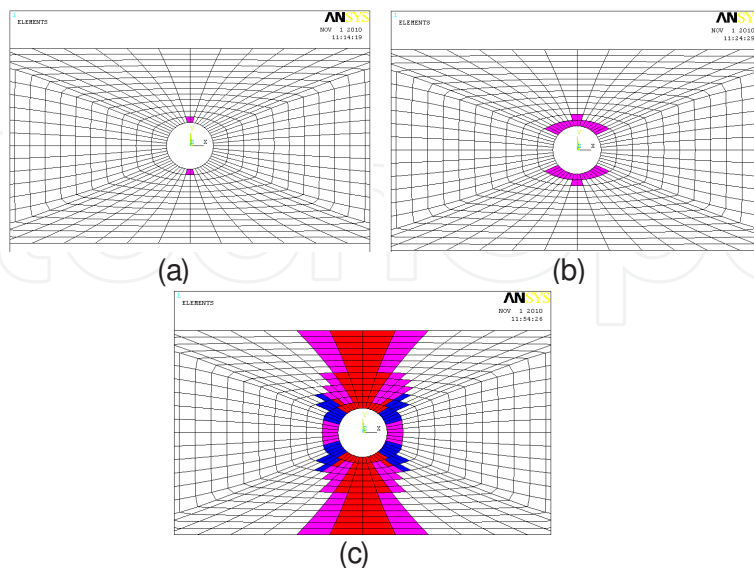


Figure 21. Failure process of plate with stress concentration at room temperature: (a) $F=2.04$ kN (FPF), (b) $F=8$ kN, (c) $F=13.72$ kN (FF)

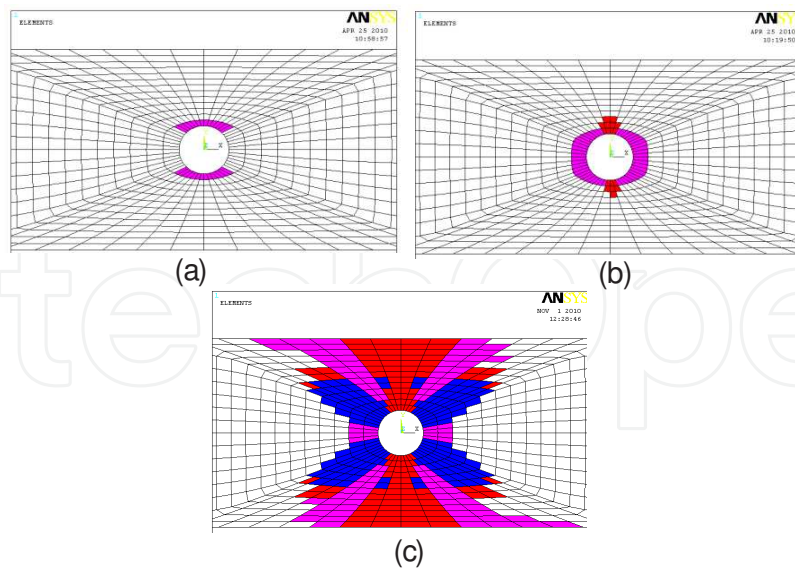


Figure 22. Failure process of plate with stress concentration at -60 °C: (a) $F=6.28$ kN (FPF), (b) $F=10$ kN, (c) $F=18.27$ kN (FF)

In all cases, major failure mode was fiber breakage, matrix cracking and fiber-matrix shearing which are shown in the figures by red, pink and blue paints respectively. Other failure modes are also occurred in the final failure but can not be shown in the figures.

Figure 23 illustrates mean values of tensile strength for quasi-isotropic laminate at room temperature and -60 °C with and without stress concentration. This figure also compares experimental results with those obtained from the present finite element model. Results show that strength of laminate increased by decreasing temperature. This is because of change of micromechanical properties of composites at low temperature.

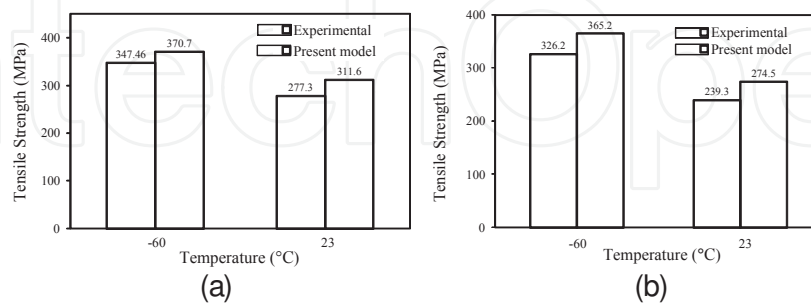


Figure 23. Tensile strength of laminates at different temperatures (a) without (b) with stress concentration

Figure 24 shows typical stress-strain curve for the laminate with stress concentration based on experimental results at room temperature and -60 °C.

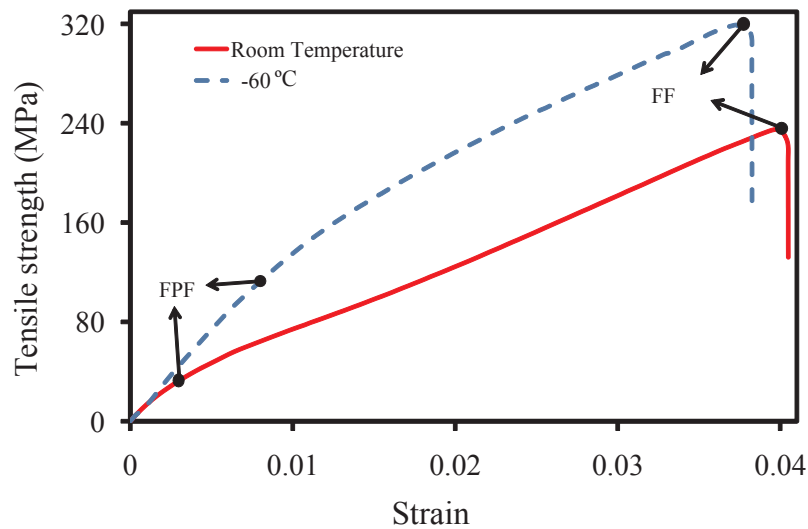


Figure 24. Typical stress-strain curve for quasi-isotropic laminate with central hole at room temperature and -60°C

Failure mechanism of tested specimens with central hole at room temperature and -60°C are different. Figure 25 shows failed specimens at two different temperatures. From a visual inspection, there is a small amount of tab de-bonding near the gage area for both two cases with more fiber pull-out for low temperature specimen. At low temperature, because of the interface between fiber and matrix are much weaker and the fiber debond from the matrix, synchronous with fiber breakage, matrix cracking and a few fiber-matrix shearing were occurred. However, the mainly failure mode for all cases is fiber breakage and matrix cracking.

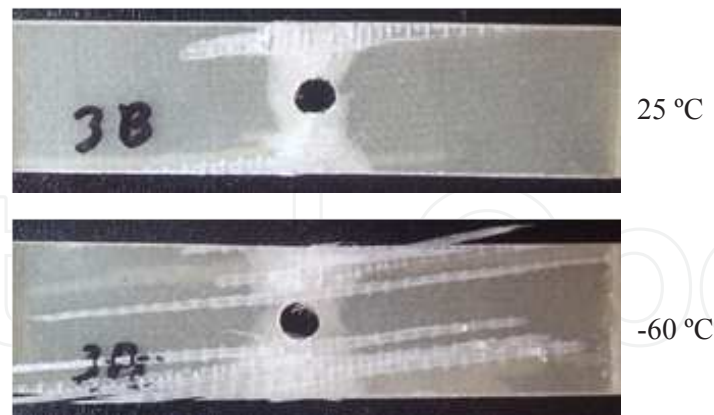


Figure 25. Failure regions of glass-fiber reinforced epoxy composites at room temperature and -60°C

7. Conclusion

Tensile failure behavior of glass/epoxy laminated composite subjected to thermo-mechanical loadings at low temperatures with/without stress concentration was investigated experimen-

tally and numerically. A finite element code was utilized to model the progressive failure analysis of quasi-isotropic composite plates at low temperatures under static loading. For each given load step, the stresses at each integration point are evaluated and the appropriate failure criterion is applied to inspect for possible failure by using Hashin failure criteria. At the point with failure, the material properties are modified according to the failure mode using a non-zero stiffness degradation factor. In case of failure detection, because of nonlinear behavior, the modified Newton–Raphson method was carried out until convergence is reached. This analysis is repeated for each load increment until the final failure occurs and the ultimate strength is determined. Based on the results of the present study, the following conclusions can be drawn:

1. The stress-strain behavior of UD laminate under tensile loads in longitudinal direction was linear elastic until breakage and the slope of the stress-strain curve and the strength increased about 12% as the temperature decreased to $-60\text{ }^{\circ}\text{C}$. On the other hand, by decreasing temperature, strain to failure decreased slightly about 10%. However, the laminate under transverse tensile loading exhibited insignificant nonlinearity (especially at room temperature) before reaching the maximum stress, which is due to the nature of the plasticity of epoxy.
2. The UD laminate showed a nonlinear elastic relation between stress and strain under compressive loads in both directions until final failure occurred catastrophically. The compressive strength increased by decreasing temperature (for longitudinal direction 28% and transverse direction 50%) while the strain to failure decreased. But in transverse direction, strain to failure increased by decreasing temperature and against other nonlinear curves, positive curvature was observed.
3. The UD laminate under in-plane shear loading behaves highly nonlinear for all temperature tests until final failure. Again, in this case, both shear strength and stiffness increased by decreasing temperature in about 32% and 70% respectively. Also nonlinear region decreased by decreasing temperature due to increasing brittleness of epoxy matrix.
4. Failure type of UD laminates under various loadings was affected by low temperature. It was found that, by decreasing temperature a small amount of tab deboning occurred near the gauge area of specimens in longitudinal tensile loading. Also, because of the interface between fiber and matrix was much weaker at low temperature, fibers deboned the matrix in all test cases. Therefore, it may be concluded that the low temperature affects the micro mechanisms of damage in composite specimen.
5. From general master curves and illustrated regression function, mechanical properties of unidirectional glass fiber polymeric composites at temperature range of $-60\text{ }^{\circ}\text{C}$ to $23\text{ }^{\circ}\text{C}$ can be evaluated.
6. The stress-strain behavior of laminate under tensile loads was linear elastic until first ply failure (FPF). After this, the behavior of laminate was nonlinear until final failure occurred. This trend was observed for laminated composite with/without stress concentration at both temperatures.

7. The slope of the stress-strain curve and the strength of laminate increased as the temperature decreased to -60°C . On the other hand, by decreasing temperature, strain to failure decreased slightly. So, in spite of improvement in strength and stiffness of composites under static loading at low temperatures in comparison with room temperature, their strain to failure under these environmental conditions becomes weaker.
8. The failure mode of laminated composite at low temperature changes from matrix cracking at FPF to mixed mode failure (fiber breakage, fiber matrix shearing and matrix cracking) at final failure load.
9. Failure type of laminates under various loadings was affected by low temperature. It was found that, by decreasing temperature a small amount of tab deboning occurred near the gage area with more fiber pull-out. Also, due to weakness of the interface between fiber and matrix at low temperature, fiber debones the matrix. Therefore, it may be concluded that the lower temperature affects the micro mechanisms of damage.
10. Good agreement was achieved between results from experimental and analytical calculation at room temperature and -60°C . This agreement also showed the validity of model.

Author details

Mohammad Amin Torabizadeh^{1*} and Abdolhossein Fereidoon²

*Address all correspondence to: Torabizadeh@yahoo.com

1 University of Applied Science and Technology, Tehran, Iran

2 University of Semnan, Semnan, Iran

References

- [1] Astm, D. D 3039M-95a, Standard test method for tensile properties of polymer matrix composite materials, (1997).
- [2] Astm, D. D 3410M-95, Standard test method for compressive properties of polymer matrix composite materials with unsupported gage section by shear loading, (1997).
- [3] Astm, D. D 4255M-83, Standard guide for testing in-plane shear properties of composite laminates, (1994).
- [4] Schutz, J. S. Properties of composite materials for cryogenic application, *Cryogenics*, 38, 3-12 ((1998).

- [5] Sun, C. T. and A. Wanki Jun, Compressive strength of unidirectional fiber composites with matrix non-linearity, *Composite Science and Technology*, (1994). , 52, 577-587.
- [6] Bechel, V. T, & Kim, R. Y. Damage trends in cryogenically cycled carbon/polymer composites, *Composite Science and Technology*. 64, 1773-1784 ((2004).
- [7] Kim, R. Y, & Donaldson, S. L. Experimental and analytical studies on the damage initiation in composite laminates at cryogenic temperature, *Composite Structure*. 76, 62-66 ((2006).
- [8] Ifju, P, Myers, D, & Schulz, W. Residual stress and thermal expansion of graphite epoxy laminates subjected to cryogenic temperatures, *Composite Science and Technology*. 66, 2449-2455 ((2006).
- [9] Rupnowski, P, Gentz, M, & Kumosa, M. Mechanical response of a unidirectional graphite fiber/polyimide composite as a function of temperature, *Composite Science and Technology*. 66, 1045-1055 ((2006).
- [10] Kim, M. G, Kang, S. G, Kim, C. G, & Kong, C. W. Tensile response of graphite/epoxy composite at low temperatures, *Composite Structures*. 79(1), 84-89 ((2007).
- [11] Takeda, T, Shindo, Y, & Narita, F. Three-dimensional thermoelastic analysis of cracked plain weave glass/epoxy composites at cryogenic temperatures, *Composite Science and Technology*. 64, 2353-2362 ((2004).
- [12] Shindo, Y, Horiguchi, K, Wang, R, & Kudo, H. Double cantilever beam measurement and finite element analysis of cryogenic Mode I interlaminar fracture toughness of glass-cloth/epoxy laminates, *Journal of Engineering Materials and Technology*. 123, 191-197 ((2001).
- [13] Melcher, R. J, & Johnson, W. S. Mode I fracture toughness of an adhesively bonded composite-composite joint in a cryogenic environment, *Composite Science and Technology*. 67(3-4), 501-6 ((2007).
- [14] Shindo, Y, Inamoto, A, & Narita, F. Characterization of Mode I fatigue crack growth in GFRP woven laminates at low temperatures, *Acta Materialia*. 53, 1389-1396 ((2005).
- [15] Shindo, Y, Inamoto, A, Narita, F, & Horiguchi, K. Mode I fatigue delamination growth in CFRP woven laminates at low temperatures, *Engineering Fracture Mechanics*. 73, 2080-2090 ((2006).
- [16] Kumagai, S, Shindo, Y, & Inamoto, A. Tension-tension fatigue behavior of GFRP woven laminates at low temperatures, *Cryogenics*. 45, 123-128 ((2005).
- [17] Shindo, Y, Takano, S, Horiguchi, K, & Sato, T. Cryogenic fatigue behavior of plain weave glass/epoxy composite laminates under tension-tension cycling, *Cryogenics*. 46, 794-798 ((2006).

- [18] Labeas, G, Belesis, S, & Stamatelos, D. Interaction of damage failure and post-buckling behavior of composite plates with cut-outs by progressive damage modeling, *Composites: Part B*. 39(2), 304-15 ((2008).
- [19] Liu, X, & Wang, G. Progressive failure analysis of bonded composite repairs, *Composite Structures*. 81, 331-340 ((2007).
- [20] Zhao, Q, Hoa, S. V, & Ouellette, P. Progressive failure of triaxial woven fabric (TWF) composites with open holes, *Composite Structures*. 65, 419-431 ((2004).
- [21] Takeda, T, Takano, S, Shindo, Y, & Nurita, F. Deformation and progressive failure behavior of woven-fabric-reinforced glass/epoxy composite laminates under tensile loading at cryogenic temperatures, *Composite Science and Technology*. 65, 1691-1702 ((2005).
- [22] Shindo, Y, Takano, S, Narita, F, & Horiguchi, K. Tensile and damage behavior of plain weave glass/epoxy composites at cryogenic temperatures, *Fusion Engineering and Design*. 81, 2479-2483 ((2006).
- [23] Akhras, G, & Li, W. C. Progressive failure analysis of thick composite plates using spline finite strip method, *Composite Structures*. 79, 34-43 ((2007).
- [24] Shokrieh, M. M, Torabizadeh, M. A, & Fereidoon, A. Progressive failure analysis of composite plates, *Proceedings of 8th Iranian aerospace society conference*. Esfahan, Iran ((2009).
- [25] ANSYSVer. 10, Canonsburg (PA): SAS IP; ((2005).
- [26] Shokrieh, M. M, Torabizadeh, M. A, & Fereidoon, A. An investigation on damage of quasi-isotropic laminated composite, *Proceedings of 18th annual international conference on mechanical engineering (In Persian)*, Tehran, Iran ((2010).
- [27] Kaw, A. W. *Mechanics of composite materials*, Taylor and Francis Group, LLC ((2006).
- [28] Shokrieh, M. M. *Progressive fatigue damage modeling of composite materials*, Ph.D. Thesis, McGill University ((1996).
- [29] Wilczynski, A. P. Longitudinal compressive strength of a unidirectional fibrous composite, *Composite Science and Technology*, (1992). , 45, 37-41.
- [30] Vogler, T. J, & Kyriakides, S. Inelastic behavior of an AS4/PEEK composite under combined transverse compression and shear. Part I: Experiments, *International Journal of Plastics*, (1999). , 15, 783-806.
- [31] Hsiao, H. M, & Daniel, I. M. Strain rate behavior of composite materials, *Composites: Part B*, (1998). , 29, 521-533.

- [32] Gonzalez, C, & Llorca, J. Mechanical behavior of unidirectional fiber-reinforced polymers under transverse compression: Microscopic mechanisms and modeling, *Composite Science and Technology*, (2007). , 67, 2795-2806.
- [33] ANSYSVer. 10, Canonsburg (PA): SAS IP; (2005).
- [34] Shokrieh, M. M, Torabizadeh, M. A, & Fereidoon, A. An investigation on damage of quasi-isotropic laminated composite," Proceedings of 18th annual international conference on mechanical engineering (In Persian), Tehran, Iran, ISME (2010).
- [35] Kaw, A. K. Mechanics of composite materials, Taylor and Francis Group, LLC, 978-0-84931-343-1(2006).
- [36] Callister, J. R. W.D., *Materials Science and Engineering: An Introduction*, Third edition, John Wiley & Sons, New York, (1994). , 480.
- [37] Nettles, A. T, & Biss, E. J. Low temperature mechanical testing of carbon-fiber/epoxy-resin composite materials, NASA Technical Paper, 3663, (1996).
- [38] Gong, M, Wang, X. F, & Zhao, J. H. Experimental study on mechanical behavior of laminates at low temperatures, *Cryogenics*, (2007). , 47, 1-7.
- [39] Walsh, R. P, Colskey, J. D, & Reed, R. P. Low temperature properties of a unidirectionally reinforced epoxy fiberglass composite, *Cryogenics*, (1995). , 35, 723-725.
- [40] Pinho, S. T, Iannucci, L, & Robinson, P. Physically-based failure models and criteria for laminated fiber-reinforced composites with emphasis on fiber-kinking. Part I: development, *Composites: Part A*, (2006). , 37, 63-73.
- [41] Puck, A, & Schurmann, H. Failure analysis of FRP laminates by means of physically based phenomenological models, *Composite Science and Technology*, (2002). , 62, 1633-1662.
- [42] Aragonés, D. Fracture micromechanisms in C/epoxy composites under transverse compression, Master thesis, Universidad Politecnica de Madrid, (2007).

IntechOpen

